

UPt₃ as a Topological Crystalline Superconductor

Yasumasa Tsutsumi,¹ Masaki Ishikawa,² Takuto Kawakami,^{2,3}
Takeshi Mizushima,² Masatoshi Sato,⁴ Masanori Ichioka,² and Kazushige Machida²

¹*Condensed Matter Theory Laboratory, RIKEN, Wako, Saitama 351-0198, Japan*

²*Department of Physics, Okayama University, Okayama 700-8530, Japan*

³*International Center for Materials Nanoarchitectonics (WPI-MANA)*

National Institute for Materials Science, Tsukuba 305-0044, Japan

⁴*Department of Applied Physics, Nagoya University, 464-8603, Japan*

(Dated: January 31, 2018)

We investigate the topological aspect of the spin-triplet f -wave superconductor UPt₃ through microscopic calculations of edge- and vortex-bound states based on the quasiclassical Eilenberger and Bogoliubov-de Gennes theories. It is shown that a gapless and linear dispersion exists at the edge of the ab -plane. This forms a Majorana valley, protected by the mirror chiral symmetry. We also demonstrate that, with increasing magnetic field, vortex-bound quasiparticles undergo a topological phase transition from topologically trivial states in the double-core vortex to zero-energy states in the normal-core vortex. As long as the \mathbf{d} -vector is locked into the ab -plane, the mirror symmetry holds the Majorana property of the zero-energy states, and thus UPt₃ preserves topological crystalline superconductivity that is robust against the crystal field and spin-orbit interaction.

PACS numbers: 74.70.Tx, 74.20.Rp

Introduction.— The unconventional aspect of the heavy-fermion superconductor UPt₃ [1] emerges as a multiple phase diagram in the temperature T vs magnetic field H plane, which is unique among a handful of strongly correlated superconductors. In low fields, UPt₃ undergoes a double superconducting transition from a normal phase to the A-phase at $T_{c1} \approx 550$ mK and from the A-phase to the B-phase at $T_{c2} \approx 500$ mK [2]. The C-phase appears in the regime of low T 's and high H 's [3, 4]. In spite of numerous works on UPt₃ over the past three decades following the discovery of superconductivity, the pairing mechanism and gap function have not been fully elucidated yet.

A recent experiment has clarified the remarkable twofold symmetry breaking of the angle-resolved thermal conductivity in the ab -plane of the C-phase [5]. This convincingly suggests a spin-triplet f -wave function belonging to the E_{1u} representation [6], where the gap function in the B-phase is described by the two-component \mathbf{d} -vector [7] and in the C-phase it reduces to a single component with the twofold symmetry breaking. Even within the B-phase, the \mathbf{d} -vector rotates from $\mathbf{d}(\mathbf{k}) \propto \lambda_a \mathbf{b} + \lambda_b \mathbf{c}$ to $\lambda_a \mathbf{b} + \lambda_b \mathbf{a}$ with increasing $\mathbf{H} \parallel \mathbf{c}$ at the critical magnetic field $H_{\text{rot}} \sim 2$ kG [8, 9], where $\lambda_{a,b}(\mathbf{k}) = k_{a,b}(5k_c^2 - k^2)$ and \mathbf{a} , \mathbf{b} , and \mathbf{c} are the unit vectors in a hexagonal crystal. Most bulk thermodynamic experiments are understandable with the E_{1u} scenario and another candidate based on the E_{2u} representation [10] described by $\mathbf{d}' \propto \mathbf{c}(k_a + ik_b)^2 k_c$ because both have point and line nodes in the B-phase [6]. The latter scenario gives rise to the spontaneous breaking of the time-reversal symmetry in the B-phase and the fourfold symmetry breaking in the C-phase. These two scenarios differ in that the multi-component order parameters originate from the multiple

\mathbf{d} -vector in the E_{1u} scenario and from the orbital degrees of freedom for the E_{2u} representation.

In this Letter, we examine topological crystalline superconductivity in the B-phase of UPt₃ appropriate for the E_{1u} scenario with multiple \mathbf{d} -vectors. On the basis of a recent idea of Majorana fermions protected by crystal point group symmetries [11–13], it is demonstrated that the nontrivial topological property is directly linked to the orientation of the \mathbf{d} -vector, and thus the field-induced rotation of the \mathbf{d} -vector is accompanied by the topological phase transition of vortex-bound states, which is not observed in the E_{2u} scenario. Here, the topological aspects are unveiled through the microscopic calculations of edge and vortex core states. It is shown that zero-energy states exist at the edge of the ab -plane, which form the topological “Majorana valley”. Furthermore, employing numerical calculations of the Bogoliubov-de Gennes (BdG) equation, we examine the discretized quantum structure of quasiparticles (QPs) bound at a double-core vortex and a normal-core vortex. It is found that increasing the magnetic field $\mathbf{H} \parallel \mathbf{c}$ induces a topological phase transition from topologically trivial states in the double-core vortex to symmetry-protected Majorana fermions in a normal-core vortex with $\mathbf{d} \perp \mathbf{c}$ via nontopological Dirac fermions. The purposes of this Letter are to help identify the pairing symmetry of UPt₃ and to place this material in the proper position of topological crystalline superconductors.

Formulation.— Here, we utilize both the quasiclassical Eilenberger theory and the BdG theory. The former is valid for $\Delta \ll E_F$, which is well satisfied for most superconductors including UPt₃, where Δ and E_F denote the pair potential and Fermi energy, respectively. The vortex-bound QP state is, however, discretized at Δ^2/E_F

intervals [14]. The BdG theory enables us to describe the full quantum structure of low-lying QPs in the vortex state.

We start with the quasiclassical spinful Eilenberger theory [6, 15–17]. The quasiclassical Green's function $\hat{g} \equiv \hat{g}(\bar{\mathbf{k}}, \mathbf{r}, \omega_n)$ is governed by the Eilenberger equation

$$-i\hbar\mathbf{v}(\bar{\mathbf{k}}) \cdot \nabla \hat{g} = \left[\begin{pmatrix} i\hbar\omega_n \hat{1} & -\hat{\Delta}(\bar{\mathbf{k}}, \mathbf{r}) \\ \hat{\Delta}^\dagger(\bar{\mathbf{k}}, \mathbf{r}) & -i\hbar\omega_n \hat{1} \end{pmatrix}, \hat{g} \right], \quad (1)$$

with the normalization condition $\hat{g}^2 = -\pi^2 \hat{1}$. The ordinary (wide) hat indicates the 2×2 (4×4) matrix in spin (particle-hole) space. The quasiclassical Green's function is described in particle-hole space by

$$\hat{g}(\bar{\mathbf{k}}, \mathbf{r}, \omega_n) = -i\pi \begin{pmatrix} \hat{g}(\bar{\mathbf{k}}, \mathbf{r}, \omega_n) & i\hat{f}(\bar{\mathbf{k}}, \mathbf{r}, \omega_n) \\ -i\hat{f}(\bar{\mathbf{k}}, \mathbf{r}, \omega_n) & -\hat{g}(\bar{\mathbf{k}}, \mathbf{r}, \omega_n) \end{pmatrix}, \quad (2)$$

with the momentum on the Fermi surface $\bar{\mathbf{k}} = \mathbf{k}/k_F = (k_a, k_b, k_c)/k_F$, the center-of-mass coordinate \mathbf{r} , and the Matsubara frequency $\omega_n = (2n + 1)\pi k_B T/\hbar$ with $n \in \mathbb{Z}$. The Fermi velocity is assumed as $\mathbf{v}(\bar{\mathbf{k}}) = v_F \bar{\mathbf{k}}$ on a three-dimensional Fermi sphere.

The spin-triplet order parameter is expressed with the \mathbf{d} -vector as $\hat{\Delta}(\bar{\mathbf{k}}, \mathbf{r}) = i\mathbf{d}(\bar{\mathbf{k}}, \mathbf{r}) \cdot \hat{\sigma}$, where $\hat{\sigma}$ is the Pauli matrix. The self-consistent condition for $\hat{\Delta}$ is given as

$$\hat{\Delta}(\bar{\mathbf{k}}, \mathbf{r}) = N_0 \pi k_B T \sum_{|\omega_n| \leq \omega_c} \left\langle V(\bar{\mathbf{k}}, \bar{\mathbf{k}}') \hat{f}(\bar{\mathbf{k}}', \mathbf{r}, \omega_n) \right\rangle_{\bar{\mathbf{k}}'}, \quad (3)$$

where N_0 is the density of states in the normal state. The cutoff energy ω_c is set to be $\hbar\omega_c = 20k_B T_c$ with the transition temperature T_c and $\langle \dots \rangle_{\bar{\mathbf{k}}}$ indicates the Fermi surface average. In the B-phase without a magnetic field, the \mathbf{d} -vector is described by $\mathbf{d} = \Delta_1 \lambda_a \mathbf{b} + \Delta_2 \lambda_b \mathbf{c}$. We neglect the splitting of T_c into T_{c1} and T_{c2} because the amplitudes of the two pair potentials, Δ_1 and Δ_2 , are nearly equal at low temperatures in the B-phase. The pairing interaction is $V(\bar{\mathbf{k}}, \bar{\mathbf{k}}') = g[\lambda_a(\bar{\mathbf{k}})\lambda_a(\bar{\mathbf{k}}') + \lambda_b(\bar{\mathbf{k}})\lambda_b(\bar{\mathbf{k}}')]$, where the coupling constant g is determined by $(gN_0)^{-1} = \ln(T/T_c) + \pi k_B T \sum_{|\omega_n| \leq \omega_c} |\hbar\omega_n|^{-1}$. We self-consistently solve Eqs. (1) and (3) at $T = 0.5T_c$.

By using the self-consistent solution of \hat{g} in Eqs. (1) and (3), the spin current is calculated as

$$\mathbf{j}_s^\mu(\mathbf{r}) = \frac{\hbar}{2} N_0 \pi k_B T \sum_{|\omega_n| \leq \omega_c} \langle \mathbf{v}(\bar{\mathbf{k}}) \text{Im}[g_\mu(\bar{\mathbf{k}}, \mathbf{r}, \omega_n)] \rangle_{\bar{\mathbf{k}}}, \quad (4)$$

where g_μ is defined as $\hat{g} = g_0 \hat{1} + \mathbf{g} \cdot \hat{\sigma}$. The local density of states (LDOS) for the energy E is given by $N(\mathbf{r}, E) = \langle N(\bar{\mathbf{k}}, \mathbf{r}, E) \rangle_{\bar{\mathbf{k}}}$, where the angle-resolved LDOS is

$$N(\bar{\mathbf{k}}, \mathbf{r}, E) = N_0 \text{Re} [g_0(\bar{\mathbf{k}}, \mathbf{r}, \omega_n)|_{i\hbar\omega_n \rightarrow E+i\eta}]. \quad (5)$$

We here introduce a positive infinitesimal constant η , which is typically fixed at $\eta = 0.007\pi k_B T_c$. To obtain

$g_0(\bar{\mathbf{k}}, \mathbf{r}, \omega_n)|_{i\hbar\omega_n \rightarrow E+i\eta}$, we solve Eq. (1) with $\eta - iE$ instead of $\hbar\omega_n$ under $\hat{\Delta}$ obtained self-consistently.

To obtain the discretized nature of vortex-bound states, we calculate the BdG equation. Since we here consider a straight vortex line along the c -axis ($\mathbf{H} \parallel \mathbf{c}$), the wave number k_c is a well-defined quantum number. The BdG equation with a definite k_c is given as [18]

$$\int d\rho_2 \begin{pmatrix} \hat{h}_{k_c}(\rho_1, \rho_2) & \hat{\Delta}_{k_c}(\rho_1, \rho_2) \\ -\hat{\Delta}_{-k_c}^\dagger(\rho_1, \rho_2) & -\hat{h}_{-k_c}(\rho_1, \rho_2) \end{pmatrix} \vec{u}_{\nu, k_c}(\rho_2) = E_{\nu, k_c} \vec{u}_{\nu, k_c}(\rho_1), \quad (6)$$

where $\hat{h}_{k_c}(\rho_1, \rho_2) = \delta(\rho_{12}) (-\hbar^2 \nabla_{2D}^2 / 2m - E_F^{2D}(k_c)) \hat{1}$ with $\nabla_{2D}^2 = \partial_a^2 + \partial_b^2$. The two-dimensional form of the Fermi energy $E_F^{2D}(k_c) = (\hbar^2 / 2m)(k_F^2 - k_c^2)$ reflects the k_c -cross section of the Fermi surface. The order parameter in Eq. (6) is obtained from the self-consistent solution of the quasiclassical theory and the relation $\hat{\Delta}_{k_c}(\rho_1, \rho_2) = (2\pi)^{-2} \int d\mathbf{k}^{2D} \hat{\Delta}(\mathbf{k}, \rho) e^{i\mathbf{k}^{2D} \cdot \rho_{12}}$, where $\rho = (\rho_1 + \rho_2)/2$, $\rho_{12} = \rho_1 - \rho_2$, and \mathbf{k}^{2D} are in the ab -plane. Equation (6) describes QPs with the energy E_{ν, k_c} and the wave function $\vec{u}_{\nu, k_c} = (u_{\nu, k_c}^\uparrow, u_{\nu, k_c}^\downarrow, v_{\nu, k_c}^\uparrow, v_{\nu, k_c}^\downarrow)^T$, where the index $\nu \in \mathbb{Z}$ denotes the ν -th excited state of Eq. (6).

Edge states.— First, using the quasiclassical theory, we consider the edge state at the surface perpendicular to the ab -plane. We here set a surface at $a = 0$ and impose the specular boundary condition on \hat{g} as $\hat{g}(\bar{\mathbf{k}}, \mathbf{r}, \omega_n) = \hat{g}(\bar{\mathbf{k}}_r, \mathbf{r}, \omega_n)$ at $a = 0$, where $\bar{\mathbf{k}}_r = \bar{\mathbf{k}} - 2\mathbf{a} \cdot \bar{\mathbf{k}}$. In the B-phase without a magnetic field, the \mathbf{d} -vector is described by $\mathbf{d}(\bar{\mathbf{k}}, a) = \Delta_\perp(a) \lambda_a(\bar{\mathbf{k}}) \mathbf{b} + \Delta_\parallel(a) \lambda_b(\bar{\mathbf{k}}) \mathbf{c}$.

The spatial profile of the order parameter along the a -axis is shown in Fig. 1(a). At $a = 0$, the specular boundary condition suppresses Δ_\perp coupled with a momentum \bar{k}_a perpendicular to the surface. In contrast, Δ_\parallel coupled to a parallel momentum \bar{k}_b is enhanced by compensating for the loss of Δ_\perp at the surface. Away from the surface, Δ_\perp increases and Δ_\parallel decreases toward the order parameter in the bulk B-phase $\Delta_0 = \Delta_\perp = \Delta_\parallel$. Figure 1(a) also shows the spin current $j_s^a(a)$, implying that the a -component of the spin flows along the b -axis on the surface.

Figure 1(b) shows LDOS at the surface ($a = 0$) and bulk ($a/R_0 = 40$), where $R_0 = \hbar v_F / (2\pi k_B T_c)$. The two peaks at $E = \Delta_0$ and $E = (16\sqrt{15}/45)\Delta_0$ in the bulk LDOS are shifted to higher energies in the surface LDOS as a result of the enhancement of Δ_\parallel at the surface. It is clearly seen that the zero-energy LDOS at the surface has substantial weight (about half of the normal state), owing to the dispersionless zero-energy state connecting point nodes at the north and south poles of the Fermi sphere, similarly to that in the superfluid $^3\text{He-A}$ [19].

We can separate the spin states by rotating the spin quantization axis to the a -axis as $\mathbf{d} = \Delta_0(\lambda_a \mathbf{b} + \lambda_b \mathbf{c}) = \Delta_0(\lambda_+ \mathbf{d}_\leftarrow + \lambda_- \mathbf{d}_\rightarrow)$, where $\lambda_\pm = \mp(\lambda_a \pm i\lambda_b)/\sqrt{2}$, $\mathbf{d}_\rightarrow = (\mathbf{b} + i\mathbf{c})/\sqrt{2}$, and $\mathbf{d}_\leftarrow = -(\mathbf{b} - i\mathbf{c})/\sqrt{2}$. In Figs. 1(c) and

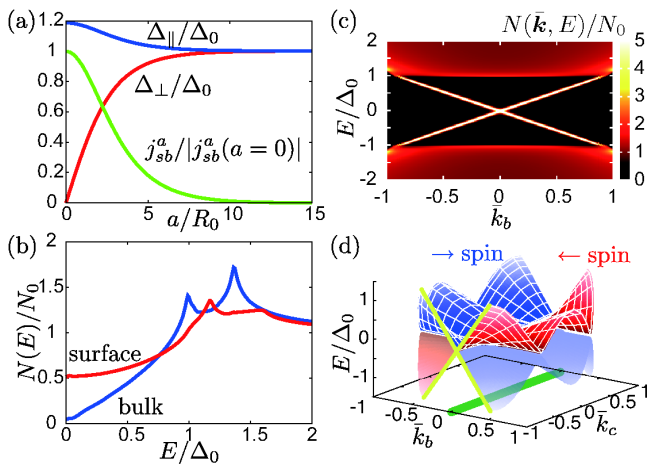


FIG. 1. (Color online) (a) Spatial profiles of order parameters and spin current j_{sb}^a along the a -axis. (b) LDOSs $N(E)$ at the surface and bulk. (c) Angle-resolved LDOS $N(\vec{k}, E)$ at the surface as a function of k_b for $k_c=0$. (d) Stereographic view of the dispersion of the surface bound state in \rightarrow - and \leftarrow -spin sectors.

1(d), we show the angle-resolved LDOS as a function of k_b for $k_c=0$ and the dispersion of the surface bound state for the \rightarrow - and \leftarrow -spin states on the k_b - k_c -plane. The energy dispersion is derived from Eq. (6) within the Andreev approximation as $E = \pm \Delta_0 |5\bar{k}_c^2 - 1| k_b$, where $+$ and $-$ correspond to the \leftarrow - and \rightarrow -spin sectors, respectively. It is found that two linear branches with opposite slopes appear inside the bulk gap. Since negative energy states are occupied at low T 's, the surface bound QPs in the \rightarrow - and \leftarrow -spin states counterflow along the $+\mathbf{b}$ and $-\mathbf{b}$ directions. Therefore, the spin current spontaneously appears along the edge of the ab -plane. The dispersion of the surface bound state forms a “Majorana valley” with a slope modulated along the k_c direction, as shown in Fig. 1(d). As is shown below, the Majorana valley in the B-phase is a direct consequence of the topological crystalline superconductivity of UPt_3 .

Vortex states.— Next, using the BdG equation Eq. (6), we clarify the vortex state under a magnetic field $\mathbf{H} \parallel \mathbf{c}$. The \mathbf{d} -vector is generalized to $\mathbf{d}(\mathbf{k}, \boldsymbol{\rho}) = \mathbf{d}_{\text{bulk}}(\mathbf{k}, \boldsymbol{\rho}) + \mathbf{d}_{\text{core}}(\mathbf{k}, \boldsymbol{\rho})$, where $\mathbf{d}_{\text{core}}(|\boldsymbol{\rho}| \rightarrow \infty) = \mathbf{0}$ denotes the component that fills the vortex core of \mathbf{d}_{bulk} . In the low- H regime of the B-phase, the bulk \mathbf{d} -vector is expressed as $\mathbf{d}_{\text{bulk}} = \Delta_0 e^{i\varphi} (\lambda_a \mathbf{b} + \lambda_b \mathbf{c})$ at $|\boldsymbol{\rho}| \rightarrow \infty$, where φ is the azimuthal angle around the vortex core from the axis $a > 0$. The normal-core vortex is characterized by $\mathbf{d}_{\text{core}} = \mathbf{0}$. The double-core vortex stabilized in the low- H and low- T regime has $\mathbf{d}_{\text{core}} = \Delta_c(\boldsymbol{\rho}) \lambda_b \mathbf{a}$ where $\Delta_c(\boldsymbol{\rho} = \mathbf{0}) \neq 0$ [6]. The momentum in \mathbf{d}_{core} is the same as that in the c -component of \mathbf{d}_{bulk} because the \mathbf{d} -vector easily rotates from the c -axis to the a -axis, as observed in the NMR Knight shift measurements [8, 9]. In the double-core vor-

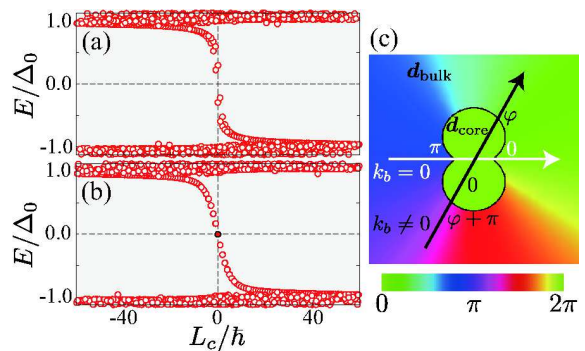


FIG. 2. (Color online) Energy spectra of QPs classified with the azimuthal angular momentum L_c at $k_c=0$: (a) double-core vortex and (b) normal-core vortex. (c) Phase profiles of \mathbf{d}_{bulk} and \mathbf{d}_{core} and quasiclassical trajectories with $k_b=0$ (white arrow) and $k_b \neq 0$ (black arrow).

tex, as seen in Fig. 2(c), the phases of $\mathbf{d}_{\text{bulk}}(\varphi=0)$ and \mathbf{d}_{core} are the same.

Figure 2(a) shows the energy spectrum of low-lying QPs in the double-core vortex with $k_c=0$, obtained from the numerical diagonalization of Eq. (6). All the eigenvalues are classified in terms of the angular momentum along the c -axis, $L_c = -i\hbar \int d\rho \bar{u}_{\nu, k_c}^\dagger (a\partial_b - b\partial_a) u_{\nu, k_c}$. It is seen from Fig. 2(a) that zero-energy eigenstates are absent even in the vicinity of $L_c=0$. To clarify the absence in the double-core vortex, let us consider the quasiclassical trajectories across the vortex core, as shown in Fig. 2(c). The quasiclassical trajectory with the momentum $k_b=0$ effectively feels the π -phase shift of the pair potential, because the induced pair potential $\mathbf{d}_{\text{core}} = \Delta_c \lambda_b \mathbf{a}$ becomes zero for $k_b=0$, where the π -phase shift is necessary for the zero-energy state. In contrast, the trajectory with $k_b \neq 0$ feels \mathbf{d}_{core} interrupting the π -phase shift, which prevents the formation of the zero-energy state. Since the QP state at the vortex core is obtained as the superposition of all the contributions of the quasiclassical trajectories with various k_b 's, the zero-energy state is absent in the double-core vortex.

The normal-core vortex with $\mathbf{d}_{\text{core}} = \mathbf{0}$ is accompanied by the spin-degenerate zero-energy modes with $L_c=0$, as shown in Fig. 2(b). Within our model, the zero-energy states form the flat band along k_c . Note that, in a magnetic field $H \sim H_{\text{rot}}$, the normal-core vortex lattice with a hexagonal symmetry is observed in the small-angle neutron scattering experiment [20]. In the regime of $H < H_{\text{rot}}$, the normal-core vortex is described by $\mathbf{d}(|\boldsymbol{\rho}| \rightarrow \infty) = \Delta_0 e^{i\varphi} (\lambda_a \mathbf{b} + \lambda_b \mathbf{c})$. The zero-energy state is found to be fragile against the Zeeman field $\mathbf{H} \parallel \mathbf{c}$ and lifted to finite energies. In the regime of $H > H_{\text{rot}}$ where $\mathbf{d}(|\boldsymbol{\rho}| \rightarrow \infty) = \Delta_0 e^{i\varphi} (\lambda_a \mathbf{b} + \lambda_b \mathbf{a})$, however, the zero-energy states with $L_c=0$ remain robust against the magnetic field along the c -axis, because the \uparrow - and \downarrow -spin sectors of the \mathbf{d} -vector can be regarded as a spinless

chiral superconductor. Hence, in the normal-core vortex, the excitation energy of the low-lying QP jumps to a zero-energy at the critical field where the \mathbf{d} -vector is locked in the ab -plane. As described below, at $H = H_{\text{rot}}$, the vortex-bound states undergo the topological phase transition associated with the mirror Chern number.

Majorana fermions protected by mirror symmetries.— Finally, we clarify the symmetry protection and the Majorana nature of zero-energy edge- and vortex-bound states in the B-phase of UPt₃. We start with the BdG Hamiltonian,

$$\widehat{\mathcal{H}}(\mathbf{k}) = \begin{pmatrix} \hat{\epsilon}(\mathbf{k}) & \hat{\Delta}(\mathbf{k}) \\ \hat{\Delta}^\dagger(\mathbf{k}) & -\hat{\epsilon}^\text{T}(-\mathbf{k}) \end{pmatrix}. \quad (7)$$

Here, $\hat{\epsilon}(\mathbf{k})$ is the Hamiltonian in the normal state of UPt₃, which holds the D_{6h} hexagonal symmetry. We find that two different mirror symmetries protect Majorana fermions in the B-phase: One is the mirror reflection $\hat{\mathcal{M}}_{ca}$ with respect to the ca -plane, which protects the Majorana valley on a surface normal to the a -axis. The other is the mirror reflection $\hat{\mathcal{M}}_{ab}$ with respect to the ab -plane, which protects the Majorana zero mode in a vortex along the c -axis. Below we show that the difference in symmetry gives rise to a difference in Majorana nature between the edge- and vortex-bound states. Note that UPt₃ shows an antiferromagnetic order in the normal state below about 5 K [21]. Even if the antiferromagnetic order coexists with the superconducting order, the mirror symmetries are preserved macroscopically beyond the scale of the coherence length.

First, we consider the symmetry protection of the surface states. Because the gap function in the B-phase is invariant under the mirror reflection $\hat{\mathcal{M}}_{ca} \propto i\hat{\sigma}_b$, the BdG Hamiltonian $\widehat{\mathcal{H}}(\mathbf{k})$ satisfies $\widehat{\mathcal{M}}_{ca}\widehat{\mathcal{H}}(\mathbf{k})\widehat{\mathcal{M}}_{ca}^\dagger = \widehat{\mathcal{H}}(k_a, -k_b, k_c)$ with $\widehat{\mathcal{M}}_{ca} \equiv \text{diag}(\hat{\mathcal{M}}_{ca}, \hat{\mathcal{M}}_{ca}^*)$. Therefore, combining the mirror symmetry with the time-reversal symmetry \mathcal{T} and the particle hole symmetry \mathcal{C} , we have ‘‘mirror chiral symmetry’’ $\{\Gamma, \widehat{\mathcal{H}}(\mathbf{k})\} = 0$ with $\Gamma = \mathcal{T}\mathcal{C}\widehat{\mathcal{M}}_{ca}$ at $k_b = 0$ [22]. The mirror chiral symmetry enables us to define the one-dimensional winding number $w(k_c) = -(4\pi i)^{-1} \int_{-\pi}^{\pi} dk_a \text{tr}[\Gamma \widehat{\mathcal{H}}^{-1} \partial_{k_a} \widehat{\mathcal{H}}]$ [23, 24], which is evaluated as $|w(k_c)| = 2$ for $k_b = 0$, $|k_c| < k_F$ and $w(k_c) = 0$ for other k_b 's and k_c 's. Thus, the system is topologically non-trivial and the bulk-edge correspondence ensures the existence of the Majorana valley in Fig. 1(d) with a flat dispersion connecting the point nodes as $E = 0$ at $k_b = 0$ and $|k_c| < k_F$. In addition, owing to the mirror chiral symmetry, the Majorana valley shows the Majorana Ising anisotropy that the surface bound states are gapped only by a magnetic field along the b -axis [25]. A magnetic field in the ca -plane or the \mathbf{d} -vector rotation in the high-field phase in the B-phase does not obscure the topological protection since the combination of the mirror reflection $\hat{\mathcal{M}}_{ca}$ and the time-reversal is not broken, but each of them is broken. Here, note that, while the Majorana valley has a close similarity to the topological Fermi arcs in

³He-A [26, 27], the arcs' topological origins are totally different: The time-reversal breaking is essential for the topological Fermi arcs, but not for the Majorana valley.

For the topological protection of zero-energy states in a vortex, the mirror reflection $\hat{\mathcal{M}}_{ab} \propto i\hat{\sigma}_c$ with respect to the ab -plane is essential. Following Ref. 11, one can show that, if the gap function is odd under the mirror reflection $\hat{\mathcal{M}}_{ab}$, $\hat{\mathcal{M}}_{ab}\hat{\Delta}(\mathbf{k})\hat{\mathcal{M}}_{ab}^\text{T} = -\hat{\Delta}(k_a, k_b, -k_c)$, a normal-core vortex may support the Majorana zero mode protected by the mirror symmetry: In this case, $\widehat{\mathcal{H}}(\mathbf{k})$ commutes with the mirror operator $\widehat{\mathcal{M}}_{ab}^{(-)} \equiv \text{diag}(\hat{\mathcal{M}}_{ab}, -\hat{\mathcal{M}}_{ab}^*)$. On the mirror reflection invariant plane $k_c = 0$, the system splits into two subsectors with two different eigenvalues of $\widehat{\mathcal{M}}_{ab}^{(-)}$, and because of the minus sign in front of $\hat{\mathcal{M}}_{ab}^*$ in the mirror operator $\widehat{\mathcal{M}}_{ab}^{(-)}$, each mirror subsector supports its own particle-hole symmetry. This means that the mirror subsectors are topologically equivalent to class D of the table in Ref. 28 and thus the nontrivial Chern number in each subsector ensures non-Abelian Majorana fermions [11, 29].

Since $\mathbf{d}(\mathbf{k}) \propto \lambda_a \mathbf{b} + \lambda_b \mathbf{c}$ does not have a definite mirror parity under $\hat{\mathcal{M}}_{ab}$, the spin-orbit interaction or crystal field, which is ignored in the numerical calculations above, lifts zero-energy states, implying that the B-phase with the configuration of such a \mathbf{d} -vector is topologically trivial for vortex-bound states. On the other hand, for $\mathbf{d}(\mathbf{k}) \propto \lambda_a \mathbf{b} + \lambda_b \mathbf{a}$ rotated by a high magnetic field $\mathbf{H} \parallel \mathbf{c}$, the gap function is odd under the mirror reflection $\hat{\mathcal{M}}_{ab}$, and Majorana vortex-bound states protected by the mirror symmetry are possible. Actually, for UPt₃ with five closed Fermi surfaces [30], the parity of the mirror Chern number at $k_c = 0$ is odd [31]. This ensures that there exist Majorana zero modes in a vortex along the c -axis. Hence, the low-lying QPs bound at the normal-core vortex undergo the topological phase transition from non-topological zero modes to symmetry protected Majorana fermions with increasing magnetic field. The topological phase transition without closing the bulk gap but accompanied by symmetry breaking has also been discussed in Refs. 25 and 32 recently.

Concluding remarks.— We have investigated the topological aspect of edge- and vortex-bound states for the recently identified gap function of the UPt₃ B-phase. In the edge state, Majorana fermions with linear dispersion are bound and their zero-energy states form the Majorana valley. The Majorana valley is protected by the mirror chiral symmetry, responsible for Ising anisotropy.

Note that the symmetry-protected Majorana valley at the surface can be detected by tunneling spectroscopy [33, 34]: The flat dispersion gives rise to a finite zero bias tunneling conductance, where the tunneling conductance is related to the surface LDOS [Fig. 1(b)] in the low transparent limit. The Majorana Ising anisotropy results in a decrease in the zero bias conductance under a magnetic field only along the b -axis. In contrast, the

surface states in the E_{2u} scenario are not coupled with a magnetic field along the b -axis.

We have also demonstrated that the double-core vortex is not accompanied by the zero-energy state. As H increases, the finite energy excitations in a double-core vortex undergo the topological transition to symmetry-protected Majorana fermions via topologically trivial zero modes in a normal-core vortex. The Majorana fermions are protected by a mirror symmetry against perturbations, such as a magnetic field, a crystal field, and a spin-orbit interaction, when the \mathbf{d} -vector is locked in the ab -plane, $\mathbf{d}(\mathbf{k}) \propto \lambda_a \mathbf{b} + \lambda_b \mathbf{a}$. Hence, the B-phase of UPt_3 offers a promising platform for studying topological crystalline superconductors.

Some of the numerical calculations were performed using the RIKEN Integrated Cluster of Clusters (RICC). This work was supported by KAKENHI (Nos. 24840048, 21340103, 22103005, 2200247703, 25287085, and 25103716).

-
- [1] G. R. Stewart, Z. Fisk, J. O. Willis, and J. L. Smith: Phys. Rev. Lett. **52** (1984) 679.
- [2] R. A. Fisher, S. Kim, B. F. Woodfield, N. E. Phillips, L. Taillefer, K. Hasselbach, J. Flouquet, A. L. Giorgi, and J. L. Smith: Phys. Rev. Lett. **62** (1989) 1411.
- [3] S. Adenwalla, S. W. Lin, Q. Z. Ran, Z. Zhao, J. B. Ketterson, J. A. Sauls, L. Taillefer, D. G. Hinks, M. Levy, and B. K. Sarma: Phys. Rev. Lett. **65** (1990) 2298.
- [4] G. Bruls, D. Weber, B. Wolf, P. Thalmeier, B. Lüthi, A. d. Visser, and A. Menovsky: Phys. Rev. Lett. **65** (1990) 2294.
- [5] Y. Machida, A. Itoh, Y. So, K. Izawa, Y. Haga, E. Yamamoto, N. Kimura, Y. Ōnuki, Y. Tsutsumi, and K. Machida: Phys. Rev. Lett. **108** (2012) 157002.
- [6] Y. Tsutsumi, K. Machida, T. Ohmi, and M. Ozaki: J. Phys. Soc. Jpn. **81** (2012) 074717.
- [7] K. Machida, T. Nishira, and T. Ohmi: J. Phys. Soc. Jpn. **68** (1999) 3364.
- [8] H. Tou, Y. Kitaoka, K. Asayama, N. Kimura, Y. Ōnuki, E. Yamamoto, and K. Maezawa: Phys. Rev. Lett. **77** (1996) 1374.
- [9] H. Tou, Y. Kitaoka, K. Ishida, K. Asayama, N. Kimura, Y. Ōnuki, E. Yamamoto, Y. Haga, and K. Maezawa: Phys. Rev. Lett. **80** (1998) 3129.
- [10] J. A. Sauls: Adv. Phys. **43** (1994) 113.
- [11] Y. Ueno, A. Yamakage, Y. Tanaka, and M. Sato: Phys. Rev. Lett. **111** (2013) 087002.
- [12] C.-K. Chiu, H. Yao, and S. Ryu: Phys. Rev. B **88** (2013) 075142.
- [13] F. Zhang, C. L. Kane, and E. J. Mele: Phys. Rev. Lett. **111** (2013) 056403.
- [14] C. Caroli, P. de Gennes, and J. Matricon: Phys. Lett. **9** (1964) 307.
- [15] G. Eilenberger: Z. Phys. **214** (1968) 195.
- [16] J. W. Serene and D. Rainer: Phys. Rep. **101** (1983) 221.
- [17] J. A. Sauls and M. Eschrig: New J. Phys. **11** (2009) 075008.
- [18] S. Kaneko, K. Matsuba, M. Hafiz, K. Yamasaki, E. Kakizaki, N. Nishida, H. Takeya, K. Hirata, T. Kawakami, T. Mizushima, and K. Machida: J. Phys. Soc. Jpn. **81** (2012) 063701.
- [19] Y. Tsutsumi, M. Ichioka, and K. Machida: Phys. Rev. B **83** (2011) 094510.
- [20] A. Huxley, P. Rodière, D. M. Paul, N. van Dijk, R. Cubitt, and J. Flouquet: Nature **406** (2000) 160.
- [21] R. H. Heffner, D. W. Cooke, A. L. Giorgi, R. L. Hutson, M. E. Schillaci, H. D. Rempp, J. L. Smith, J. O. Willis, D. E. MacLaughlin, C. Boekema, R. L. Lichti, J. Oostens, and A. B. Denison: Phys. Rev. B **39** (1989) 11345.
- [22] T. Mizushima and M. Sato: New J. Phys. **15** (2013) 075010.
- [23] M. Sato and S. Fujimoto: Phys. Rev. B **79** (2009) 094504.
- [24] M. Sato, Y. Tanaka, K. Yada, and T. Yokoyama: Phys. Rev. B **83** (2011) 224511.
- [25] T. Mizushima, M. Sato, and K. Machida: Phys. Rev. Lett. **109** (2012) 165301.
- [26] G. E. Volovik: J. Supercond. Nov. Magn. **26** (2013) 2887.
- [27] M. A. Silaev and G. E. Volovik: Phys. Rev. B **86** (2012) 214511.
- [28] A. P. Schnyder, S. Ryu, A. Furusaki, and A. W. W. Ludwig: Phys. Rev. B **78** (2008) 195125.
- [29] M. Sato, A. Yamakage, and T. Mizushima: to be published in Physica E; arXiv:1305.7469.
- [30] G. J. McMullan, P. M. C. Rourke, M. R. Norman, A. D. Huxley, N. Doiron-Leyraud, J. Flouquet, G. G. Lonzarich, A. McCollam, and S. R. Julian: New J. Phys. **10** (2008) 053029.
- [31] M. Sato: Phys. Rev. B **81** (2010) 220504.
- [32] M. Ezawa, Y. Tanaka, and N. Nagaosa: Sci. Rep. **3** (2013) 2790.
- [33] Y. Tanaka and S. Kashiwaya: Phys. Rev. Lett. **74** (1995) 3451.
- [34] S. Kashiwaya and Y. Tanaka: Rep. Prog. Phys. **63** (2000) 1641.